AIAA JOURNAL
Vol. 44, No. 9, September 2006

Aeroelastic Optimization of a Helicopter Rotor Using Orthogonal Array–Based Metamodels

Smita Bhadra* and Ranjan Ganguli†
Indian Institute of Science, Bangalore 560 012, India

Aeroelastic optimization of a four-bladed, soft-inplane hingeless rotor is performed to reduce hub loads and blade root loads with blade stiffness design variables. An aeroelastic analysis based on the finite element method is used. Aerodynamic modeling includes a time domain unsteady aerodynamic model and a free wake model. Metamodels (models of models) of the aeroelastic analysis are investigated in a systematic manner including various experimental designs such as factorial designs, central composite designs (CCD), gradient-enhanced CCD, and orthogonal arrays (OA). Linear, quadratic, and cubic polynomial response surfaces are obtained, and graphical, statistical, and optimization results obtained are used to compare the different designs. It is found that the CCD and OA are able to capture the basic trends of the analysis using sequential second-order polynomial response surfaces and are further investigated for use in optimization. However, the OA, which is a fractional factorial design, requires significantly fewer analysis runs than the CCD. Numerical results obtained for single-objective and multiobjective optimization problems show a 16–22% reduction in vibratory hub loads for a nonuniform blade with six elastic stiffness design variables. The multiobjective optimization problem based on the min–max method reduces the vibratory hub loads by about 16% and the 1/rev and 2/rev blade root loads, which are the principal cause of dynamic stresses, by about 18 and 31%, respectively. The OA-based metamodels provide an efficient and interactive approach to perform preliminary design studies using comprehensive simulation codes and is suitable for use in an industrial setting.

Nomenclature

C_d	=	blade section drag coefficient
C_l	=	blade section lift coefficient
C_m	=	blade section moment coefficient
C_T	=	thrust coefficient
c	=	blade chord
EI_y	=	flap bending stiffness
EI_z	=	lag bending stiffness
F	=	hub forces
F_x	=	longitudinal hub force
F_y	=	lateral hub force
F_z	=	vertical hub force
GJ	=	torsion stiffness
grad@mp	=	gradient calculated at point with lowest function value
grad@cp	=	gradient calculated at the center point of the design
J	=	objective function for vibration
Jd_1, Jd_2	=	objective function for dynamic stresses
k	=	number of independent variables, design variables
M	=	hub moments
M_x	=	rolling moment
M_y	=	pitching moment
M_z	=	yawing moment
N_b	=	number of blades
P	=	order of the response surface polynomial
R	=	rotor radius
R^2, R^2-adj	=	measures of verifying model adequacy
v	=	lag bending deflection of blade
w	=	flap bending deflection of blade
α	=	location of axial points, angle of attack
β_i	=	regression parameters
ζ	=	damping
μ	=	advance ratio
ϕ	=	torsion deformation of blade
σ	=	solidity ratio
γ	=	Lock number
Ω	=	rotation speed
$()^{4\Omega}$, $()^{1\Omega}$, $()^{2\Omega}$	=	4Ω, 1Ω, 2Ω component
$()^{\text{low}}$	=	lower bound of design variable
$()^{\text{high}}$	=	upper bound of the design variable

Received 28 June 2004; revision received 21 June 2005; accepted for publication 29 January 2006.

*Graduate Student, Department of Aerospace Engineering; currently Graduate Student, Alfred Gessow Rotorcraft Center, University of Maryland, College Park, MD 20742.

†Associate Professor, Department of Aerospace Engineering. Senior Member AIAA.

Introduction

VIBRATION reduction remains a key focus of helicopter research.[1,2] Passive vibration devices are routinely used to suppress vibration levels at some selected place in the helicopter body, but the major drawbacks with the passive vibration devices are a large weight penalty and rapid performance degradation away from the tuned flight condition.[3,4] Again, active vibration control methodology has also received increased attention in recent years due to the advent of smart materials.[5,6] However, active approaches have cost and reliability problems. An alternative approach is to design a low-vibration rotor using optimization methods.[7–28] However, optimization methods are difficult to use in the helicopter industry because the process of integrating optimization algorithms with simulation codes is very time consuming and cumbersome. These difficulties can be addressed by the use of metamodels, which are simple approximations to the expensive computer analysis and are therefore models of models. Metamodels have been widely used in structural and fixed-wing optimization[28–34] but need to be systematically studied for the helicopter optimization problems. The systematic study and application of metamodels for rotor optimization is the primary focus of this work.

The rotor design problem is highly complex and multidisciplinary in nature, because the flexibility of the main rotor blades are coupled with the aerodynamics, dynamics, and control systems. Early studies solved the rotor optimization problems using

gradient-based optimization methods.[8] Because of high computer time requirements, analytical derivatives have been used in several studies.[9–11] Analytical sensitivity calculations are even more important for problems involving aeroservoelasticity[12] and flight mechanics.[13,14] A wide range of design variables including blade mass and structural properties,[15,16] aerodynamic properties,[2] composite ply angles,[10,17] and advanced blade geometry[18,19] have been used. Some researchers have used optimization methods to improve aeromechanical stability,[20] place actuators on the helicopter airframe to reduce vibrations,[21] and design a rotor with trailing edge flaps.[22] Selected studies have also used nongradient methods such as genetic algorithms.[23,24] A recent review on helicopter optimization is provided by Ganguli.[25]

Almost all of these studies are academic and do not address some key issues that occur in industry environment where optimization methods need to be ultimately used. In industry, comprehensive helicopter aeroelastic codes are often proprietary and it is difficult to make changes inside them. Therefore, the use of analytical or semianalytical derivatives is difficult. In addition, finite difference–based approaches are very time consuming for helicopter optimization, and appropriate selection of step size for finite difference is not easy.

These problems led to the use of approximation techniques. Approximation techniques have been used in helicopter optimization problems.[18,26] The use of an that smoothing model helps in filtering out this numerical noise. However, the Taylor's series approximations that are typically used are only locally valid. Response surface methods are global approximations and are valid in a much larger region compared to Taylor's series. A major advantage of the use of the response surface method in optimization is the decoupling of the analysis and optimization problems. Very limited work has been done on the use of response surface methods for helicopter optimization. Ganguli[27] used response surface for helicopter rotor optimization. A major contribution of this study was the decoupling of the analysis problem and the optimization problem. The objective of the improved design was to reduce vibrating loads at the rotor hub, because they are the main source of helicopter vibration. The study used only one response surface–based iteration and quasi-steady aerodynamics with linear inflow. Murugan and Ganguli[28] extended this approach using a sequence of response surface approximations. The design variables considered in the study were the blade stiffnesses and the mass of the blade. This study included unsteady aerodynamic modeling. In both studies, only the central composite design was used to construct second-order polynomial approximations of rotor vibration. In addition, free wake aerodynamics was not used and these studies were limited in terms of simulation fidelity. Free wake inflow modeling is necessary for the accurate prediction of helicopter vibratory hub loads. The helicopter aeroelastic problem is nonlinear due to the presence of Coriolis forces and moderate deflections. The inclusion of a free wake inflow model can further increase the nonlinear effects. Most past studies did not use free wake modeling because of computer time issues. However, if we are able to develop high-quality metamodels with relatively fewer analysis runs, it is possible to use computationally expensive free wake models for helicopter optimization. Note that one of the key motivators of the metamodels in fixed-wing optimization is the use of computational fluid dynamics (CFD), which greatly increases the computational cost of traditional optimization approaches.

The techniques of design of experiments, response surface methodology, and Taguchi methods used for the construction of metamodels are investigated in this paper for application to the rotor design problem. Selected references in this area are discussed. Simpson et al. present a detailed survey on the use of metamodels for computer-based engineering simulations.[29]

Response surfaces are polynomial approximations to the analysis problem. In an early paper, Roux et al.[30] used response surfaces to construct approximations for structural optimization. Three design optimization problems that are considered benchmark problems of structural optimizations were investigated. The experimental points for all of the approximations were chosen based on the D-optimality criterion. The authors concluded that, first, though the accuracy of the response surface can be increased by increasing the number of experimental points, it is ultimately limited by the choice of approximating function. Second, the strongest determinant of accuracy was found to be the domain of approximation. So the authors recommended a windowing strategy with a series of small regions. Typically, second-order polynomials are used for response surfaces. However, some studies have also used higher-order polynomial approximations. Venter and Haftka[31] investigated the use of response surface approximations to overcome the numerical noise and software integration problems associated with complex optimization problems.

Other researchers have recently used gradient information to enhance the quality of the response surface. Chung and Alonso[32] used both function values and their gradients with respect to the design variables in the problem to construct the response surface. This reduces the number of design points and hence the number of runs of the numerical experiment in their study. A CFD analysis was used in this work. However, this approach is advantageous only when the gradients can be obtained through inexpensive algorithms. Some attempts have been made to develop a systematic approach to the selection of response surfaces. Romero et al.[33] examined the different data fitting and interpolation techniques to construct a sequence of progressively upgraded response surface approximations based on progressive lattice sampling (PLS) incremental designs. The techniques used for data fitting were finite element interpolation, polynomial regression, and kriging. A test problem was considered to examine the accuracy. An increasing levelwise accuracy for the average fitting error was observed with all schemes. Also, the performance of the polynomial regression leveled off after a certain level, after which the performance of the polynomial could not be improved by adding more points. A major contribution of the study was the use of PLS as an efficient approach for generating suitable incremental experimental designs.

One problem with response surfaces methods based on the design of experiments is the requirement of a large number of sampling points as the number of variable increases. This problem can be alleviated to some extent by the use of orthogonal arrays. Orthogonal arrays are simple fractional factorial designs and are used to reduce the number of design points. They have been widely used for quality control; however, they also appear to be useful for constructing approximate models. Unal et al.[34] studied the response surface for computer experiments using the orthogonal arrays. The use of orthogonal array constructed for computer experiments (OACE) for response surface methods did not show any advantage over the use of a three-level Taguchi orthogonal array. The results obtained were the same in both cases. The author concluded that this might be due to the fact that the design variables could take only the three discrete values. Therefore, from this study it can be inferred that the use of orthogonal arrays themselves can be sufficient when variables can take only discrete values. Khoei et al.[35] used orthogonal arrays for developing a robust design method for aluminum recycling process. The orthogonal array technique was described for experimental design because it reduces the number of experiments required to investigate a set of parameters and to minimize time and cost while performing experiments. Analysis of variance was used to determine the optimal point in this study. Similarly, Lee et al.[36] used orthogonal arrays iteratively for structural optimization in discrete design space. Analysis of mean was used in this study to determine the new design in a certain iteration. One of the problems considered was that of a 10-bar truss. The results were compared to those obtained from using genetic algorithms (GA) for the same problem, and the number of function evaluations required using the given methodology was found to be almost one-tenth of the number required using GA.

In this study, we look at constructing metamodels using response surfaces for helicopter vibration for use in rotorcraft optimization. The main new contributions of the paper are 1) the use of high-fidelity aeroelastic simulation including free wake aerodynamics that was not used in earlier studies,[27,28] resulting in more accurate capture of the nonlinear dependence between vibration and the structural design variables; 2) a systematic evaluation of 10 different

design-of-experiment approaches for the helicopter rotor vibration approximation to identity the best approach in terms of efficiency and accuracy leading to the identification of Taguchi orthogonal array as a powerful technique for rotor optimization; and 3) the use of multiobjective optimization based on the min–max method to combine vibration and dynamic stress objective functions. Note that the comparison and demonstration of the current metamodeling methods on problems as complex as the rotor problem has not been done in the literature. The results in this work will help in spreading the use of optimization methods in the rotorcraft industry.

Experimental Designs

A computer experiment is a number of runs of a computer model or simulation code.[37] The main feature of a computer experiment that distinguishes it from the physical experiment is the absence of random error, that is, the output is deterministic. However, because running a code involves expensive computational time, the selection of inputs at which to run the computer code for efficient prediction of the output is an experimental design problem. An experimental design represents a sequence of experiments to be performed, expressed in terms of design variables set at specified levels. The experimental design is represented by the matrix X, where the rows of this matrix denote the experiment runs and columns denote particular factor settings.

The most basic design is the full factorial design. The number of design points dictated by a full factorial design is the product of the number of levels for each factor. In the present study, 2^k and 3^k designs are used. The number of evaluations required increases exponentially with the number of factors so to investigate the quadratic effects a central composite design, or a Box–Benkhen design can be used. Central composite designs (CCD) are a class of designed experiments that were devised specifically for fitting second-order response surfaces. These designs consist of 2^k factorial designs augmented by $2k$ axial points and one center point. Each of the independent variables is scaled such that each of the 2^k factorial points lies at the vertices of a k-dimensional hypercube and each of $2k$ axial points lies at a distance α from the center of the factorial design, where $\alpha = \sqrt{k}$. The data points are therefore evaluated at five levels of each variable, given as $(-\alpha, -1, 0, 1, \alpha)$. In the face-centered CCD design, the axial points lie on the walls of the hypercube, i.e., $\alpha = 1$. The face-centered CCD allows easy applications of move limits in the hypercube region and is used in this study. A detailed description of CCD and Box–Benkhen is given by Montgomery.[38]

The limitation of time and computation costs preclude the use of CCD or even 2^k design for a large k. Therefore, to efficiently and economically investigate the design factors, fractional factorial experiment (FFE) designs are used. FFE, as the name suggests, uses only a fraction of the total number of possible combinations to estimate the main factor effects and some of the interactions. Taguchi has developed a family of FFEs, known as Taguchi's orthogonal arrays, that can be used in various situations. Orthogonality here implies that the factors can be evaluated independently of one another.[39] In the present study the Taguchi L_4, L_9, and L_{18} orthogonal arrays are used.

Response Surface Methodology

After the experimental design and necessary runs of the computer experiment, the next step for construction of a metamodel is the choice of a fitting method. For the present study, regression models are used to fit the data and construct response surfaces for the objective function. Response surface methodology (RSM) is a collection of mathematical and statistical techniques that are useful for modeling of problems.[40] Response surfaces are smooth analytical functions that are most often approximated by low-order polynomials. The approximation can be expressed as

$$y(x) = f(x) + \epsilon \tag{1}$$

where $y(x)$ is the unknown function of interest, $f(x)$ is a known polynomial function of x, and ϵ is random error. If the response is well modeled by a linear function of the k independent variables, then the approximating function is the first-order model

$$y = \beta_0 + \beta_1 x_1 + \beta_2 x_2 + \cdots + \beta_k x_k + \epsilon \tag{2}$$

When nonlinearities are present, a second-order model is used:

$$y = \beta_0 + \sum_{i=1}^{k} \beta_i x_i + \sum_{i=1}^{k} \beta_{ii} x_i^2 + \sum \sum_{i<j} \beta_{ij} x_i x_j + \epsilon \tag{3}$$

The parameters β_0, β_i, β_{ii}, and β_{ij} of the polynomials in Eqs. (2) and (3) are determined through least-squares regression, which minimizes the sum of the squares of the deviations of predicted values, $\hat{y}(x)$, from the actual values, $y(x)$. For example, the second-order response surface for two design variables is

$$y(x_1, x_2) = \beta_0 + \beta_1 x_1 + \beta_2 x_2 + \beta_{11} x_1^2 + \beta_{12} x_1 x_2 + \beta_{22} x_2^2 \tag{4}$$

To evaluate the parameters β_0, etc., Eqs. (2) and (3) can be written as

$$y = X\beta + \epsilon \tag{5}$$

where y is a $n \times 1$ vector of responses and X is a $n \times p$ matrix of sample data points as

$$X = \begin{bmatrix} 1 & x_{11} & x_{12} & x_{11}^2 & x_{12}^2 & x_{11}x_{12} \\ 1 & x_{21} & x_{22} & x_{21}^2 & x_{22}^2 & x_{21}x_{22} \\ . & . & . & . & . & . \\ . & . & . & . & . & . \\ 1 & x_{n1} & x_{n2} & x_{n1}^2 & x_{n2}^2 & x_{n1}x_{n2} \end{bmatrix} \tag{6}$$

Here β is a $p \times 1$ vector of the regression parameters, ϵ is a $p \times 1$ vector of error terms, and p is the number of design points. The parameters β_0, β_i, β_{ii}, and β_{ij} are obtained by minimizing the least-square error obtained using Eq. (5) (Ref. 40):

$$L = \sum_{i=1}^{n} \epsilon_i^2 = \epsilon^T \epsilon = (y - X\beta)^T (y - X\beta)$$

$$= y^T y - 2\beta^T X^T y + \beta^T X^T X \beta \tag{7}$$

where L is the square of the error. To minimize L, Eq. (7) is differentiated with respect to β:

$$\left.\frac{\partial L}{\partial \beta}\right|_{\hat{\beta}} = -2X^T y + 2X^T X\hat{\beta} = 0$$

$$\text{or} \qquad \hat{\beta} = (X^T X)^{-1} X^T y \tag{8}$$

Therefore, the fitted regression model is

$$\hat{y} = X\hat{\beta} \tag{9}$$

Problem Formulation

The UMARC code[41] is used for the aeroelastic analysis. The analysis is based on finite elements in space and time. A coupled trim procedure is used to solve the rotor blade response and trim equations simultaneously. The blade loads are calculated using the force summation method. Details of the analysis are given in Refs. 27 and 41.

The objective function used is the scalar norm of the forces and moments transmitted by the rotor to the fuselage, which is the principal source of vibration. An N_b-bladed rotor transmits $N_b\Omega$ forces and moments to the fuselage. Hence, for the four-bladed rotor considered in this case, the objective function is[25]

$$J = \sqrt{\left(F_x^{4\Omega}\right)^2 + \left(F_y^{4\Omega}\right)^2 + \left(F_z^{4\Omega}\right)^2}$$

$$+ \sqrt{\left(M_x^{4\Omega}\right)^2 + \left(M_y^{4\Omega}\right)^2 + \left(M_z^{4\Omega}\right)^2} \tag{10}$$

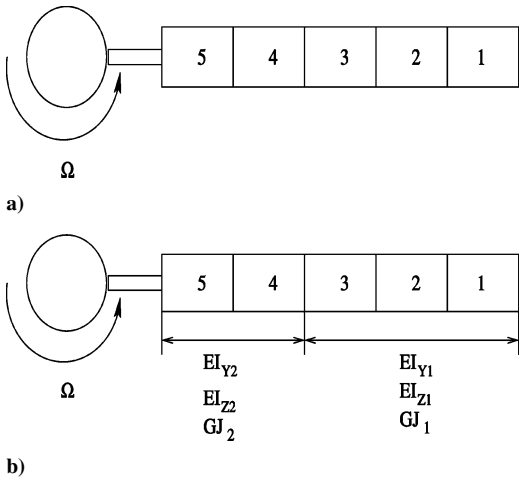

Fig. 1 Schematic representation of a) blade divided into five uniform beam elements, three design variables and b) nonuniform beam elements, six design variables.

The move limits are

$$EI_y^{(\text{low})} \le EI_y \le EI_y^{(\text{high})} \tag{11}$$

$$EI_z^{(\text{low})} \le EI_z \le EI_z^{(\text{high})} \tag{12}$$

$$GJ^{(\text{low})} \le GJ \le GJ^{(\text{high})} \tag{13}$$

The higher and lower bounds on the elastic stiffness design variables are selected at 25% greater and lower than the baseline design. Because vibratory hub loads are dependent on the aerodynamic modeling, a free wake model and unsteady aerodynamic models are used.

The first step in this study is the comparison of various response surface approaches. The objective is to find the best approximation in terms of accuracy while using the least number of analysis computations. Note that helicopter aeroelastic analysis with the free wake model may result in a considerably nonlinear variation of the vibratory hub loads objective function. This nonlinearity could be greater than that occurring in fixed-wing applications. A straightforward use of the considerable work done using response surfaces for fixed-wing problems to rotary-wing problems is not possible. Therefore, a systematic study of the nature of the vibration design space for rotary-wing problems is needed.

Study of Design Space

To examine the nature of the design space, the rotor blade is divided into five uniform beam elements as in Fig. 1a, and each of the design variables is divided using a 10×10 grid. The analysis is now run at each of the grid points for two design variables, keeping the third fixed at the baseline value. A spline fit is done using the results obtained. A spline fit model fits the points exactly and interpolates the values within them; hence it can be inferred that the spline fit using the results at 100 points in the design space can give a good idea of the true nature of the design space.

Investigation of Different Experimental Designs

To obtain the best approximation in terms of accuracy and fewest analysis computations, response surfaces (linear, quadratic, and cubic) are constructed using various experimental designs and compared on the basis of accuracy and the optimal point obtained. The different experimental designs that are examined are as follows:

1) Progressive lattice sampling method (PLS).[33] This involves upgrading the experimental design by increasing the number of points in the design space and at the same time retaining the points of the previous design. A two-dimensional PLS sequence is shown in Fig. 2. Starting from a 2^k design, $2^2 = 4$ points, a face-centered CCD is constructed by adding the axial points and a center point: $2^2 + 2 \times 2 + 1 = 9$ points. A 3^k design is generated from this by adding the midpoints of the edges as in a Box–Benkhen design, $3^2 = 9$ points. For two variables the CCD and 3^k are identical. Proceeding from a 3^k design, a subscaled 2^k is formed within the design space with half the perturbation of the full-scale design, and thus the number of points increase to $3^2 + 2^2 = 13$ points.

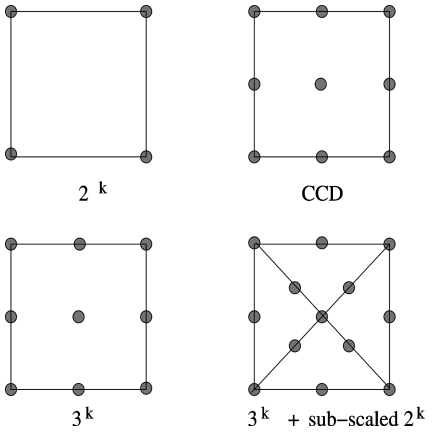

Fig. 2 Progressive lattice sampling method.

2) Use of gradient information. Gradients can be used to increase the accuracy of response surfaces. The gradient of the function is evaluated with respect to the design variables using the finite difference method, and the values are used in the construction of the response surface. Two cases of the gradient-enhanced design are considered. In one case the gradient is evaluated at the center point. In the second case, the gradient is evaluated at the point at which the value of the objective function is lowest. This is done to examine whether the gradient of the function improves the accuracy of the fit. Because finite difference calculation of gradient is computationally expensive, the number of points of the gradient evaluation is kept at a minimum of one.

In the case of the gradient-enhanced response surface method, the regression parameters of Eq. (3) are calculated as

$$\hat{\beta} = (X^T W X)^{-1} X^T W y \tag{14}$$

Here W is the weighting matrix,[32] which is taken as the identity matrix in the present study. For a two-design-variable problem of quadratic response surface, y and X are defined as

$$y = \{y_1 \;\; y_2 \;\; \cdots \;\; y_n \;\; g_{11} \;\; g_{12}\}^T \tag{15}$$

where $[y_1, y_2, \ldots y_n]$ are the values of the response at the design points, n being the number of design points depending on the experimental design used. Here, g_{11} and g_{12} are the gradients of the response at point 1 with respect to design variable 1 and 2, respectively. The augmented X is given as

$$X = \begin{bmatrix} 1 & x_{11} & x_{12} & x_{11}^2 & x_{12}^2 & x_{11}x_{12} \\ 1 & x_{21} & x_{22} & x_{21}^2 & x_{22}^2 & x_{21}x_{22} \\ \cdot & \cdot & \cdot & \cdot & \cdot & \cdot \\ \cdot & \cdot & \cdot & \cdot & \cdot & \cdot \\ 1 & x_{n1} & x_{n2} & x_{n1}^2 & x_{n2}^2 & x_{n1}x_{n2} \\ 0 & 1 & 0 & 2x_{11} & 0 & x_{12} \\ 0 & 0 & 1 & 0 & 2x_{12} & x_{11} \end{bmatrix} \tag{16}$$

3) Use of Taguchi's orthogonal arrays. A problem with the factorial designs is the rapid growth in the number of points where analysis needs to be conducted as the number of design variables increase. For example, the factorial and CCD designs are governed by the number 2^k. There is also 3^k design, which is even more computationally expensive. Orthogonal arrays provide an ordered approach to conduct numerical experiments with a fraction of the designs required for the factorial design. The L_4 and L_9 designs

Table 1 L_4 orthogonal array

	Factors		
Experiment number	$x_1(EI_y)$	$x_2(EI_z)$	$x_3(GJ)$
1	−1	−1	−1
2	−1	1	1
3	1	−1	1
4	1	1	−1

Table 2 L_9 orthogonal array

	Factors		
Experiment number	$x_1(EI_y)$	$x_2(EI_z)$	$x_3(GJ)$
1	−1	−1	−1
2	−1	0	0
3	−1	1	1
4	0	−1	0
5	0	0	1
6	0	1	−1
7	1	−1	1
8	1	0	−1
9	1	1	0

Table 3 L_{18} orthogonal array

Experiment number	Factors					
	$x_1(EI_{y1})$	$x_2(EI_{y2})$	$x_3(EI_{z1})$	$x_4(EI_{z2})$	$x_5(GJ_1)$	$x_6(GJ_2)$
1	−1	−1	−1	−1	−1	−1
2	−1	0	0	0	0	0
3	−1	1	1	1	1	1
4	0	−1	−1	0	0	1
5	0	0	0	1	1	−1
6	0	1	1	−1	−1	0
7	1	−1	0	−1	1	1
8	1	0	1	0	−1	−1
9	1	1	−1	1	0	0
10	−1	−1	1	1	0	−1
11	−1	0	−1	−1	1	0
12	−1	1	0	0	−1	1
13	0	−1	0	1	−1	0
14	0	0	1	−1	0	1
15	0	1	−1	0	1	−1
16	1	−1	1	0	1	0
17	1	0	−1	1	−1	1
18	1	1	0	−1	0	−1

are used to examine the accuracy of the fit with fewer experimental runs. The orthogonal arrays for three design variables with two and three levels used in the present study are given in Tables 1 and 2, respectively. Table 3 gives the orthogonal array with six design variables and three levels.

The different approximations are compared on the basis of 1) R^2-adjusted values and 2) root mean square error (RMSE) at randomly selected points in the design space and at the grid points evaluated for building the spline fit model.

Random points are generated at $N = 10$ points inside the design space using a random number generator. The RMSE is calculated at these points as a measure of accuracy of the fit as follows:

$$\text{RMSE} = \left[\sum_{i=1}^{N} \frac{(y_i - \hat{y}_i)^2}{N} \right]^{\frac{1}{2}} \tag{17}$$

where y_i is the response from the analysis and $\hat{y}_i$ is the response from the metamodel. The factor R^2 is a measure of the amount of reduction in the variability of the objective function obtained by using the regressor variables, and R^2-adjusted takes into account the number of parameters in the model. They are calculated as follows:

$$R^2 = \frac{SS_R}{SS_T} = 1 - \frac{SS_E}{SS_T} = 1 - \frac{y^T y - b^T X^T y}{y^T y - \left(\sum_{i=1}^{n} y_i\right)^2 / n} \tag{18}$$

$$R^2\text{-adj} = 1 - \frac{n-1}{n-p}(1 - R^2) \tag{19}$$

Based on this comparison some designs are selected for further investigation.

Results and Discussion

For the present study, a four-bladed soft-inplane hingeless rotor similar to the BO-105 rotor is considered. The baseline rotor properties are shown in Table 4. The dimensionless elastic stiffnesses are taken as design variables. The rotor blade is divided into five beam elements as in Fig. 1a, and 10 modes are used for trim analysis. The blade steady response is calculated by dividing the azimuth into six time elements with a fifth-order polynomial distribution within each element. Results are obtained in forward flight at an advance ratio of 0.3 and $C_T/\sigma = 0.07$. For aeroelastic analysis, the aerodynamic model based on nonlinear inflow and reverse flow is considered.

Comparison of Experimental Designs

Initial results are obtained with three design variables (EI_y, EI_z, GJ) for the uniform blade. A metamodel was developed for the objective function J, relating it to the three design variables. The metamodel was then used for unconstrained optimization of J with move limits on the design variables at ±25% as shown in Eqs. (10–13). The optimization is performed using the sequential quadratic algorithm (SQP) in MATLAB. The exact analysis is then performed at the optima obtained to assess the reduction in the objective function. The results for the accuracy of the fit along with the optimization results are given in Table 5. In this case it is seen that that the value of R^2-adj increases from the linear to the quadratic model but decreases for the case of the cubic model, which indicates that quadratic terms are necessary but the cubic terms do not add value. The results obtained using orthogonal arrays for selection of design points and using derivative information at the center and minimum point is given in Table 6. It is observed that the quadratic approximation using the face-centered CCD gives the best point in terms of the optimal point. Using the spline fit model data, the root mean square (rms) error due to the metamodels are calculated and presented in Table 7. It is observed that compared to linear models the error is less for quadratic and cubic models. However, compared to quadratic model the amount of reduction in error obtained using cubic model is marginal. Also, the reduction in error by using more points, e.g., 3^k and 3^k augmented by a subscaled 2^k design, is marginal compared to the increased number of analysis runs required. The objective here is to obtain the optima with fewer analysis runs. Therefore, for the problem of determination of the optimal point, the model obtained using the CCD design seems to be accurate. However, because in a CCD the number of runs increases almost exponentially with the number of design variables, the use of Taguchi orthogonal arrays, such as L_9, also seems to be an attractive design option because of the smaller number of runs. Hence, the CCD and L_9 designs are used in a sequence for the determination of the global optimum.

Table 4 Rotor properties

Parameter	Value
Number of blades	4
Radius, m	4.94
Hover tip speed, m/s	198.12
C_l	6.0α
C_d	$0.0060 + 0.20\alpha^2$
C_m	0.0000
c/R	0.055
σ	0.10
C_T/σ	0.07
γ	5.2
m_0	6.46
$EI_y/m_0\Omega^2R^4$	0.0108
$EI_z/m_0\Omega^2R^4$	0.0268
$GJ/m_0\Omega^2R^4$	0.00615
Precone β_P	0.0

Table 5 Comparison of factorial and central composite experimental designs

Design	P	Accuracy (RMSE) Random points	R^2-adj	Optimization EI_y	EI_z	GJ	Active constraints	Reduction in J, %
2^k	1	0.2968	0.9959	0.0135	0.0335	0.0046	3	2.54
CCD	2	0.1517	0.9990	0.0114	0.0301	0.0046	1	5.12
3^k	2	0.1516	0.9972	0.0112	0.0301	0.0046	1	5.04
3^k + subscaled2^k	2	0.1315	0.9180	0.0110	0.0297	0.0049	0	4.51
3^k	3	0.1081	0.9983	0.0112	0.0287	0.0046	1	3.85
3^k + subscaled2^k	3	0.0520	0.9842	0.0111	0.0335	0.0061	0	3.6

Table 6 Comparison of orthogonal arrays and gradient enhanced designs

Design	P	Accuracy (RMSE) Random points	Optimization EI_y	EI_z	GJ	Active constraints	Reduction in J, %
L_4	1	0.2922	0.0135	0.0335	0.0046	3	2.54
L_9	2	0.1483	0.0135	0.0305	0.0046	2	1.69
CCD + grad@cp	2	0.2844	0.0135	0.0322	0.0046	2	2.43
CCD + grad@mp	2	0.1865	0.0133	0.0335	0.0046	2	3.18

Table 7 Comparison of metamodels based on RMSE

Design	P	RMSE EI_y at baseline	EI_z at baseline	GJ at baseline
2^k	1	0.3516	0.3093	0.3438
CCD	2	0.2763	0.0166	0.2847
3^k	2	0.2768	0.0184	0.2848
3^k + subscaled2^k	2	0.2633	0.0364	0.2710
3^k	3	0.2543	0.0150	0.2738
3^k + subscaled2^k	3	0.2351	0.0351	0.2581
L_4	1	0.3470	0.3054	0.3440
L_9	2	0.2722	0.0145	0.2879
CCD + grad@cp	2	0.3967	0.1100	0.3627
CCD + grad@mp	2	0.2834	0.1003	0.2617

Sequence of Response Surfaces

For the determination of the global optimum, a recommended approach is the use of response surfaces in a sequence.[30] Based on the results obtained, the CCD and the OA designs appear to give the best combination of accuracy and relatively low number of design points. Therefore, for these models a sequence of response surface approximations is constructed, using the optimal point from the first design as the baseline for the next and so on. The higher and lower bounds on the elastic stiffness are reduced sequentially from 25 to 5% in five iterations with a reduction of 5% in each iteration. The optimal points obtained from each of the models along with the number of function evaluations are now compared. The optimization results obtained are given in Tables 8 and 9. Here, three sets of results are shown with different starting points, at the baseline design, upper bound, and lower bound. Very similar optimal points are obtained. Note that the response surface may smooth out deep local minima, which may not be robust to perturbations in design variables. Thus it can be concluded that the optimal points located by the response surface are generally robust. From the optimization results, it can be inferred that although the CCD gives better optimal point in the first iteration itself, the global optima as obtained from both designs are similar after the five iterations. The total number of function evaluations needed using CCD is 75, whereas for the L_9 design it is 45. Therefore, for a large number of variables the orthogonal array seems to be a more advantageous design. However, the orthogonal arrays used here have fewer points than the number of regression coefficients in the polynomial response surface model. Mathematically, the orthogonal arrays provide cruder approximations than the CCD designs. Therefore, additional numerical experiments are needed before making any conclusions about the use of OA for the response surface approximations for this problem. To study this, the number of design variable is increased by considering a nonuniform blade.

Nonuniform Blade: Six Design Variables

The number of design variables is increased to six, making the beam nonuniform, as shown in Fig. 1b. Two blade segments are considered with 40% at the root and 60% outboard. This is a more realistic approximation of a real blade with smeared finite element properties. The performance of the experimental design models is again examined to select the model that offered appreciable reduction in objective function along with a lesser number of function calls. The orthogonal array used for this problem is the L_{18} orthogonal array with 18 experiment runs and 8 factors.[35] Six factor columns are chosen, and the orthogonal array as used in the present investigation is shown in Table 3. The values from 18 runs are used along with the value for the baseline design.

The results of this problem are given in Table 10 and Table 11. Again, three different starting points are considered. A reduction of above 20% is obtained using orthogonal arrays in four iterations, and that required 18×4, that is, 72 runs, whereas in the case of CCD, the four iterations required 77×4, that is, 328 runs of the simulation code, to give a similar reduction in the objective function. Note that the designs using CCD and OA are different, showing they are improved designs only compared to the baseline and are not optimal in the mathematical sense. However, for engineering design purposes what is of interest is the vibration reduction obtained, which is about the same in both cases. Because the OA design is much more efficient than the CCD, the OA is used for future investigations. The different starting points with the OA give three somewhat different designs, yielding almost the same vibration reduction of 22–23%. The flap stiffness is almost identical for the three starting points. The lag stiffness is identical for the designs starting from baseline and upper bound but somewhat different for the design starting from the lower bound. The torsion stiffness is different for the three cases. The frequencies corresponding to these designs are shown in Table 12. The variation of frequency of the rotor blade in the preceding cases is $1.09\Omega - 1.16\Omega$ for the flap mode, $0.64\Omega - 0.80\Omega$ for the lag mode, and $4.07\Omega - 5.07\Omega$ for the torsion mode. These frequencies also lie in the range that is desirable of typical hingeless soft-inplane rotors. Therefore, the optimal design obtained by using the orthogonal array is acceptable. Again, by examining frequencies for the L_{18} designs in Table 12, it can be observed that the design starting from the upper bound has a torsion frequency of about 4.07Ω, which is close to 4Ω. The design starting from the

Table 8 Optimization results using L_9 orthogonal array

	Optimization starting point					
	Baseline		Upper bound		Lower bound	
Sequence number	Optimal point $[EI_y \ EI_z \ GJ]$	Reduction in J, %	Optimal point $[EI_y \ EI_z \ GJ]$	Reduction in J, %	Optimal point $[EI_y \ EI_z \ GJ]$	Reduction in J, %
1	[0.0135 0.0305 0.0046]	1.7	[0.010 0.0301 0.0077]	1.06	[0.0135 0.0305 0.0046]	1.7
2	[0.0117 0.0349 0.0047]	5.78	[0.0117 0.0350 0.0047]	5.77	[0.0117 0.0348 0.0047]	5.78
3	[0.0112 0.0334 0.0047]	5.75	[0.0113 0.0327 0.0048]	5.54	[0.0113 0.0333 0.0047]	5.75
4	[0.0115 0.0342 0.0047]	5.84	[0.0113 0.0357 0.0046]	5.94	[0.0114 0.0351 0.0046]	5.97
5	[0.0115 0.0342 0.0047]	5.84	[0.0114 0.0356 0.0045]	5.98	[0.0114 0.0343 0.0046]	5.96

Table 9 Optimization results using CCD

	Optimization starting point					
	Baseline		Upper bound		Lower bound	
Sequence number	Optimal point $[EI_y \ EI_z \ GJ]$	Reduction in J, %	Optimal point $[EI_y \ EI_z \ GJ]$	Reduction in J, %	Optimal point $[EI_y \ EI_z \ GJ]$	Reduction in J, %
1	[0.0114 0.0301 0.0046]	5.12	[0.0117 0.0303 0.0077]	2.5	[0.0114 0.0301 0.0046]	5.12
2	[0.0113 0.0334 0.0048]	5.59	[0.0113 0.0334 0.0048]	5.59	[0.0113 0.0334 0.0048]	5.61
3	[0.0112 0.0343 0.0048]	5.58	[0.0112 0.0343 0.0048]	5.58	[0.0112 0.0344 0.0048]	5.58
4	[0.0112 0.0344 0.0048]	5.58	[0.0111 0.0354 0.0047]	5.74	[0.0115 0.0335 0.0047]	5.81
5	[0.0115 0.0335 0.0047]	5.81	[0.0113 0.0347 0.0046]	5.96	[0.0116 0.0331 0.0046]	5.85

Table 10 Optimization results using L_{18} orthogonal array for six variables

	Optimization starting point					
	Baseline		Upper bound		Lower bound	
Sequence number	Optimal point $[EI_{y1} \ EI_{z1} \ GJ_1]$ $[EI_{y2} \ EI_{z2} \ GJ_2]$	Reduction in J, %	Optimal point $[EI_{y1} \ EI_{z1} \ GJ_1]$ $[EI_{y2} \ EI_{z2} \ GJ_2]$	Reduction in J, %	Optimal point $[EI_{y1} \ EI_{z1} \ GJ_1]$ $[EI_{y2} \ EI_{z2} \ GJ_2]$	Reduction in J, %
1	[0.0081 0.0285 0.0077]	8.69	[0.0135 0.0335 0.0046]	9.96	[0.0081 0.0285 0.0077]	8.69
	[0.0135 0.0335 0.0077]		[0.0081 0.0201 0.0077]		[0.0135 0.0335 0.0077]	
2	[0.0162 0.0402 0.0037]	15.76	[0.0162 0.0402 0.0037]	15.76	[0.0162 0.0402 0.0037]	15.76
	[0.0065 0.0171 0.0105]		[0.0065 0.0171 0.0105]		[0.0065 0.0171 0.0105]	
3	[0.0186 0.0462 0.0031]	19.80	[0.0186 0.0462 0.0043]	19.30	[0.0186 0.0462 0.0031]	19.80
	[0.0055 0.0162 0.0134]		[0.0055 0.0171 0.0118]		[0.0055 0.0162 0.0134]	
4	[0.0205 0.0508 0.0028]	22.90	[0.0205 0.0508 0.0034]	21.96	[0.0205 0.0488 0.0028]	23.45
	[0.0049 0.0169 0.0104]		[0.0049 0.0167 0.0164]		[0.0049 0.0173 0.0079]	

Table 11 Optimization results using CCD for six variables

	Optimization starting point					
	Baseline		Upper bound		Lower bound	
Sequence number	Optimal point $[EI_{y1} \ EI_{z1} \ GJ_1]$ $[EI_{y2} \ EI_{z2} \ GJ_2]$	Reduction in J, %	Optimal point $[EI_{y1} \ EI_{z1} \ GJ_1]$ $[EI_{y2} \ EI_{z2} \ GJ_2]$	Reduction in J, %	Optimal point $[EI_{y1} \ EI_{z1} \ GJ_1]$ $[EI_{y2} \ EI_{z2} \ GJ_2]$	Reduction in J, %
1	[0.0117 0.0279 0.0061]	4.71	[0.0117 0.0279 0.0061]	4.71	[0.0117 0.0279 0.0061]	4.71
	[0.0100 0.0335 0.0062]		[0.0100 0.0335 0.0062]		[0.0100 0.0335 0.0062]	
2	[0.0140 0.0335 0.0049]	13.51	[0.0140 0.0335 0.0049]	13.51	[0.0140 0.0335 0.0049]	13.51
	[0.0080 0.0313 0.0049]		[0.0080 0.0313 0.0049]		[0.0080 0.0313 0.0049]	
3	[0.0161 0.0385 0.0048]	17.75	[0.0161 0.0375 0.0052]	17.70	[0.0161 0.0382 0.0044]	17.81
	[0.0068 0.0310 0.0048]		[0.0068 0.0319 0.0045]		[0.0068 0.0302 0.0051]	
4	[0.0177 0.0398 0.0045]	20.34	[0.0177 0.0398 0.0045]	20.27	[0.0177 0.0381 0.0041]	20.31
	[0.0061 0.0294 0.0048]		[0.0061 0.0300 0.0046]		[0.0061 0.0286 0.0049]	

Table 12 Frequencies of optimal designs for six design variables using L_{18} OA along with the baseline frequencies

	Rotating frequencies (per rev), starting point		
Design	Baseline [lag flap torsion]	Upper bound [lag flap torsion]	Lower bound [lag flap torsion]
Baseline	[0.7438 1.1457 4.5508]	[0.7438 1.1457 4.5508]	[0.7438 1.1457 4.5508]
Single objective	[0.6438 1.0987 4.2627]	[0.6485 1.0987 4.0716]	[0.6414 1.0987 4.8525]
Multiobjective	[0.5838 1.0987 6.2368]	[0.5838 1.0987 6.2368]	[0.5838 1.0987 6.2368]

lower bound has a high torsion stiffness of 4.85Ω. Therefore, the design starting from the baseline appears most suitable for use. The optimization approach using approximations thus allows interactive use of engineering judgment in selecting the optimal designs.

Multiobjective Optimization

The problems that have been considered in the preceding sections are concerned with a single objective function, that is, the reduction of vibration alone. But it is desirable to reduce vibrations and dynamic stresses together. One approach is to minimize the vibration objective function with constraints on the dynamic stresses. A better approach is to consider a multiobjective problem and minimize all of the objective functions. The min–max approach represents a useful way to solve multiobjective optimization problems.[42] The scalar norm of the 1/rev and 2/rev blade root loads are used to define the objective functions for the dynamic stresses as they are the principal cause of dynamic stresses. The objective functions can thus be expressed as

$$Jd_1 = \sqrt{\left(F_x^{1\Omega}\right)^2 + \left(F_y^{1\Omega}\right)^2 + \left(F_z^{1\Omega}\right)^2} + \sqrt{\left(M_x^{1\Omega}\right)^2 + \left(M_y^{1\Omega}\right)^2 + \left(M_z^{1\Omega}\right)^2} \tag{20}$$

$$Jd_2 = \sqrt{\left(F_x^{2\Omega}\right)^2 + \left(F_y^{2\Omega}\right)^2 + \left(F_z^{2\Omega}\right)^2} + \sqrt{\left(M_x^{2\Omega}\right)^2 + \left(M_y^{2\Omega}\right)^2 + \left(M_z^{2\Omega}\right)^2} \tag{21}$$

The multiple objective problem can now be stated as follows:

$$\text{Minimize} \quad J = [J, Jd_1, Jd_2] \tag{22}$$

$$\text{Subject to} \quad EI_y^{(\text{low})} \le EI_y \le EI_y^{(\text{high})}$$
$$EI_z^{(\text{low})} \le EI_z \le EI_z^{(\text{high})}$$
$$GJ^{(\text{low})} \le GJ \le GJ^{(\text{high})} \tag{23}$$

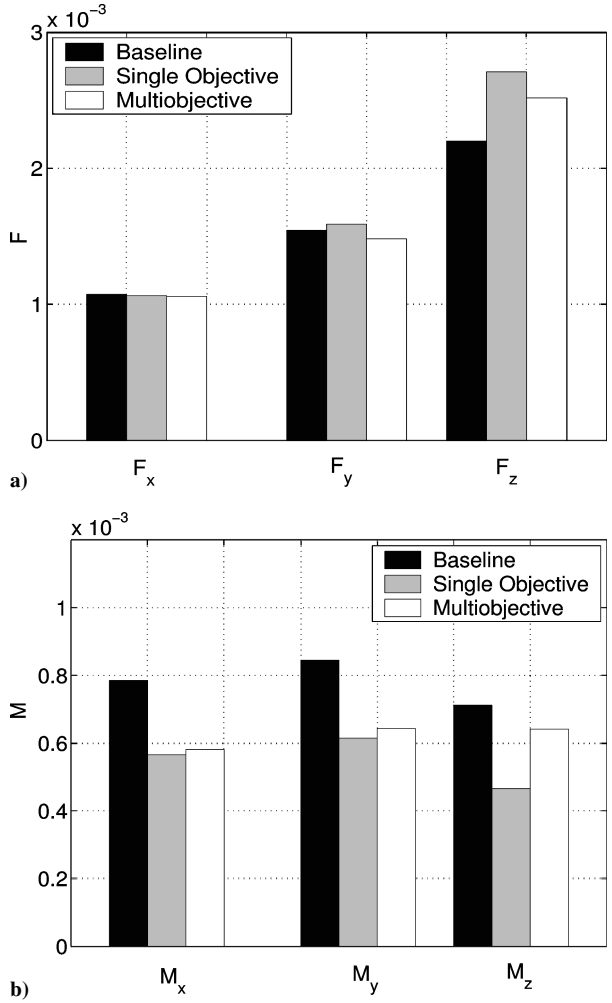

Fig. 3 Comparison of 4/rev hub loads: a) forces and b) moments for six-variable optimal designs.

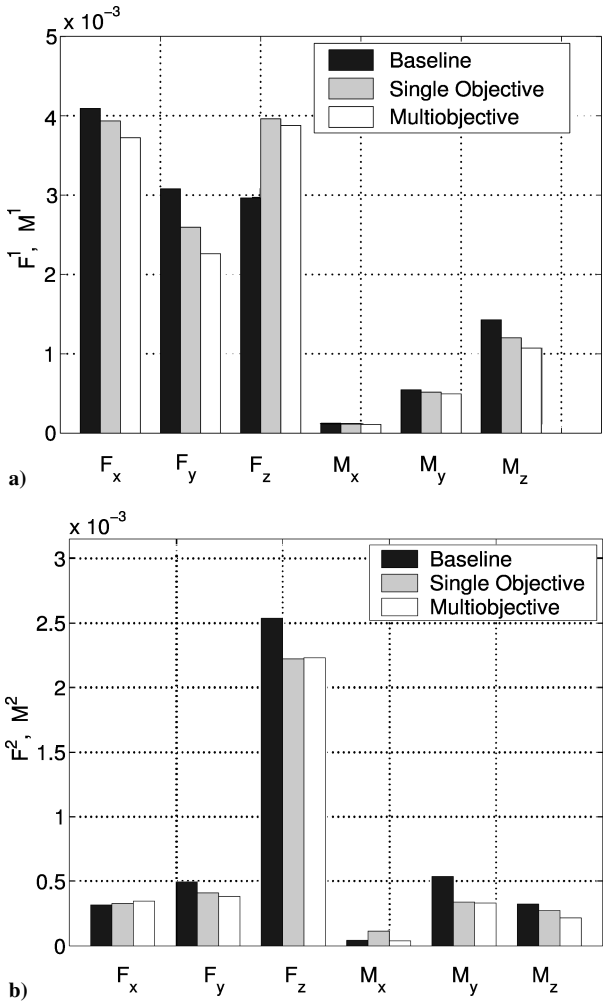

Fig. 4 Comparison of rotating frame loads: a) first harmonic and b) second harmonic for six-variable optimal designs.

Table 13 Multiobjective optimization results using L_{18} orthogonal array for six variables

Sequence number	Optimization: Optimal point $[EI_{y1}\ EI_{z1}\ GJ_1]$	Optimization: Optimal point $[EI_{y2}\ EI_{z2}\ GJ_2]$	Reduction, % J	Reduction, % Jd_1	Reduction, % Jd_2
1	[0.0135 0.0335 0.0077]	[0.0081 0.0201 0.0077]	8.92	8.04	13.70
2	[0.0162 0.0402 0.0092]	[0.0065 0.0161 0.0092]	13.38	13.03	22.18
3	[0.0186 0.0462 0.0106]	[0.0055 0.0137 0.0106]	15.51	15.95	27.48
4	[0.0205 0.0508 0.0117]	[0.0049 0.0123 0.0117]	16.22	17.64	30.67

Let $J^{\min}$, $Jd_1^{\min}$, $Jd_2^{\min}$ be the minimum of each objective function of Eq. (22). Then, the deviation from the best values can be defined as

$$z_1 = |J - J^{\min}| \tag{24}$$

$$z_2 = \left|Jd_1 - Jd_1^{\min}\right| \tag{25}$$

$$z_3 = \left|Jd_2 - Jd_2^{\min}\right| \tag{26}$$

In the min–max approach, the optimal point is determined such that the maximum deviation is minimized, that is,

$$\min[\max\{z_1, z_2, z_3\}] \tag{27}$$

subject to the move limits as in Eq. (23). The deviations z_i, $i = 1, 2, 3$, are normalized with respect to their respective minimum function values.

The results of the multiobjective optimization problem for the six-design-variable case are given in Table 13. Here, the same optimal design is obtained for all the starting points.

Study of Final Designs

For the unconstrained L_{18} OA problem, the design obtained by starting from the baseline design is used along with the final optimal design obtained from the multiobjective problem. From Tables 10 and 13 it is observed that the final reduction in the value of the vibration objective function J is less in case of the multiobjective problem (16%) compared to the unconstrained single-objective problem (23%). However the reduction in the rotating frame loads is more in

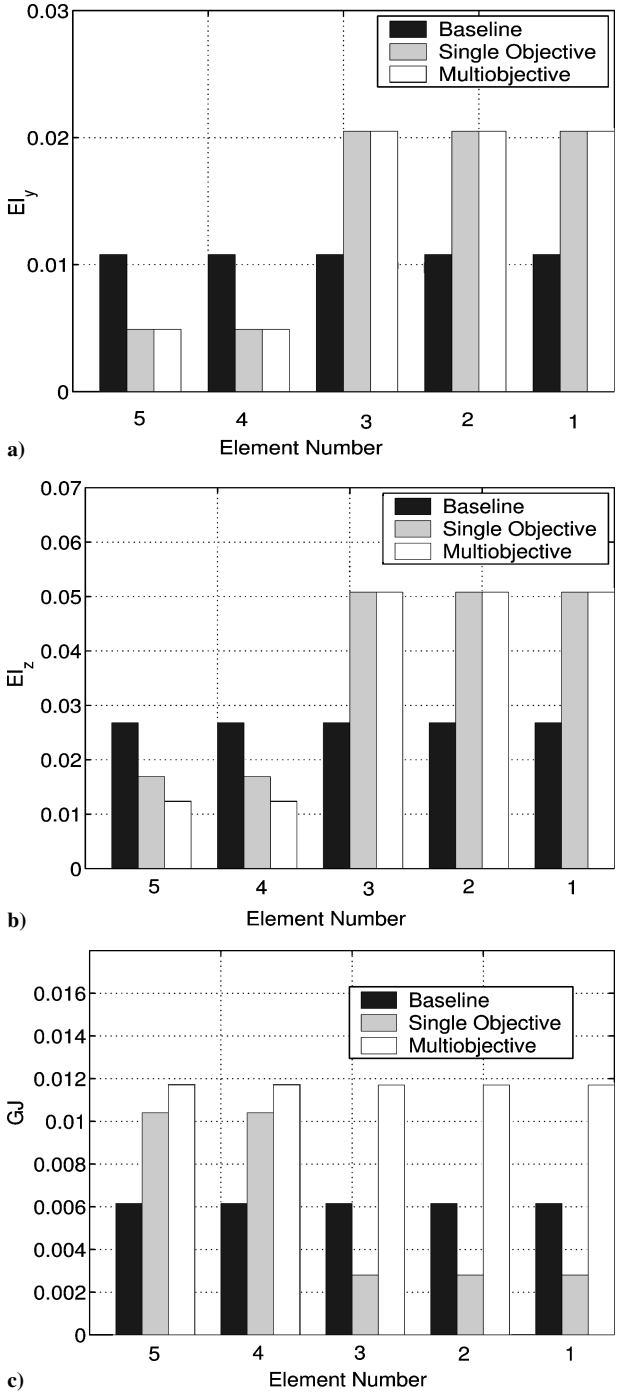

Fig. 5 Stiffness in a) flap, b) lag, and c) torsion for six-variable optimal designs.

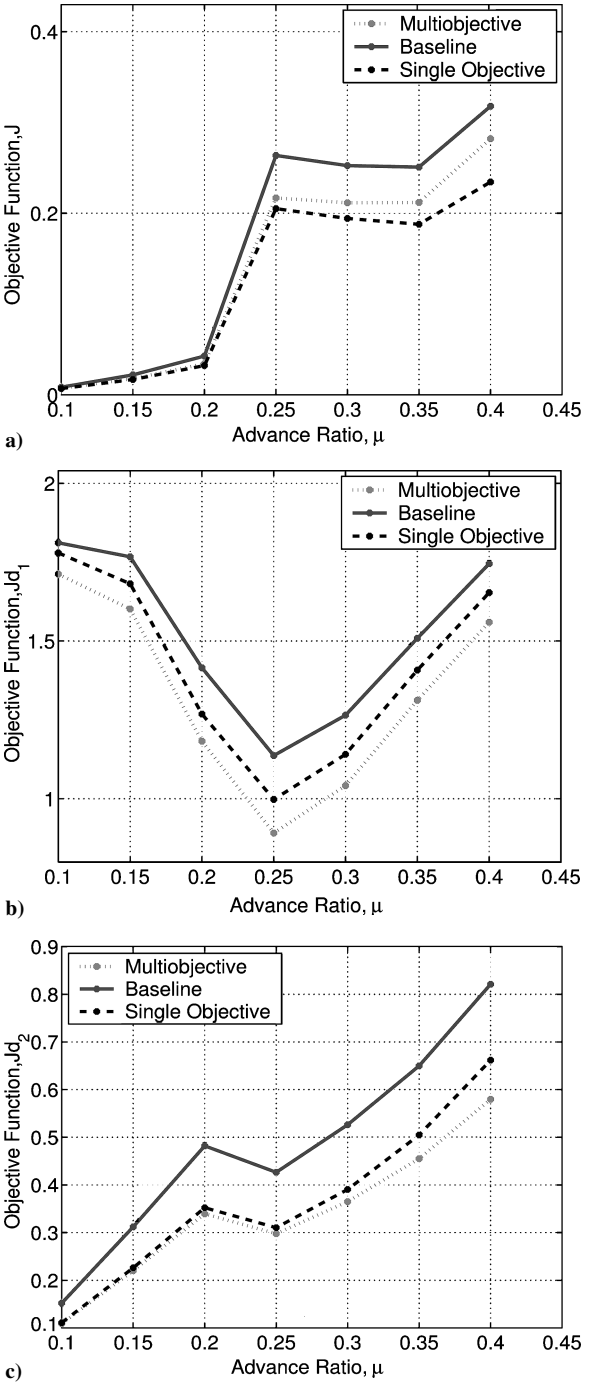

Fig. 6 Comparison of a) J, b) Jd_1, and c) Jd_2 at different advance ratios μ.

the multiobjective case. The reduction in the rotating frame loads, Jd_1 and Jd_2, in the case of the single-objective problem are 10 and 25%, respectively, whereas in the case of the multiobjective design it is 18 and 31%, respectively. Therefore, it can be observed that a greater reduction in rotating frame loads is obtained at the cost of lesser reduction in the hub loads.

The 4/rev hub loads shown in Fig. 3 point to a substantial decrease in the 4/rev moments. However, the 4/rev forces show small change and the 4/rev vertical shear increases slightly. The 1/rev and 2/rev loads are shown in Fig. 4. It is observed that in the case of the first harmonic, the loads of the design with six design variables have decreased in comparison to the baseline design except for load F_z. The multiobjective design results in a greater reduction of the blade loads compared to the unconstrained design. For the second harmonic, most forces and moments are smaller compared to the baseline design. The multiobjective design again tends to reduce the blade loads more compared to the single-objective design.

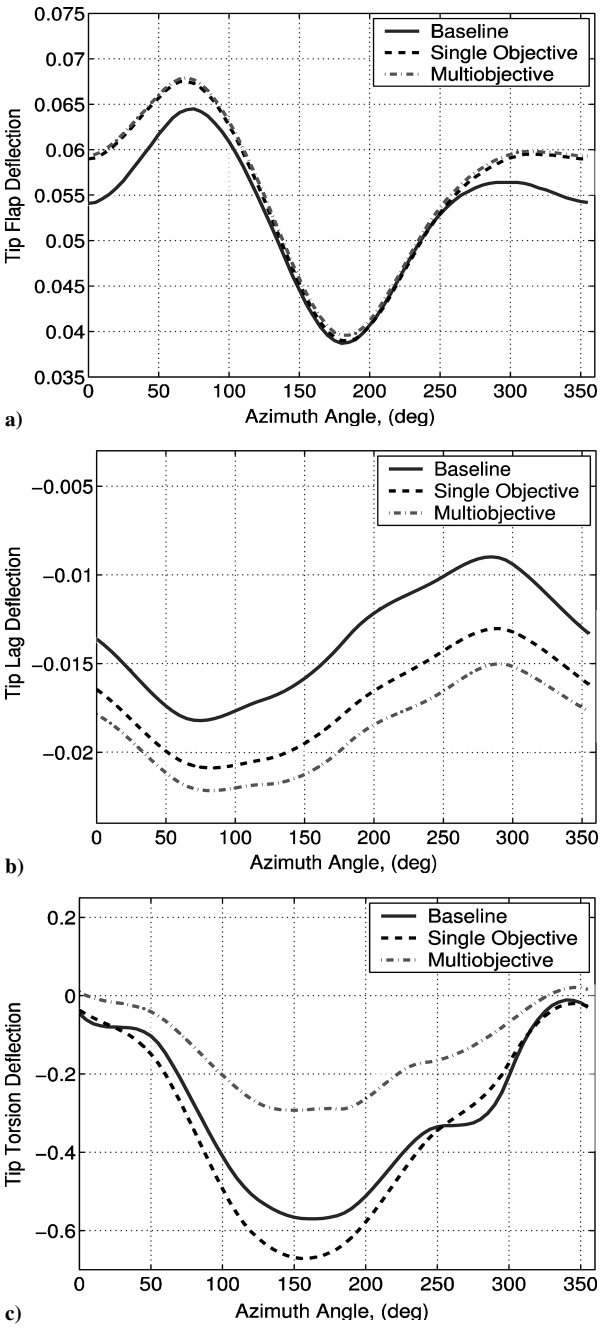

Fig. 7 Variation of tip deflection in a) flap, b) lag, and c) torsion directions along the azimuth.

The flap, lag, and torsion stiffness for these designs along with the baseline design is shown in Fig. 5. For the flap stiffness EI_y it is observed that for the six-design-variable case, the stiffness requirement near the root, elements 4 and 5, has decreased and the stiffness required at the outboard sections has increased considerably for both the single-objective and multiobjective designs. For the lag stiffness EI_z, it is observed that again the stiffness requirement near the root has decreased and the stiffness at the tip has increased for the single-objective design. In the case of the multiobjective design, the stiffness requirement in the inboard sections has decreased further. For the torsion stiffness GJ in the case of the single-objective design, the stiffness near the root has increased and has decreased for the outboard elements, whereas in the case of the multiple criterion design the torsion stiffness requirement has increased considerably and uniformly along the beam.

A comparison of the variation of the objective functions with advance ratios for the baseline and optimal design is shown in Fig. 6. It is observed that a substantial reduction in all of the objective functions is obtained using both optimal designs at higher advance ratios. However, the reduction in the vibration reduction objective function J is reduced in the case of the multiobjective design as a result of a larger reduction in the dynamic load objective functions Jd_1 and Jd_2. The aeromechanical stability is also examined. To examine the aeromechanical stability, the least damped mode is investigated; this mode is a regressive lag mode. It is observed that the single-objective design is less stable ($\zeta = 0.24$) and the multiobjective design is more stable ($\zeta = 0.27$) compared to the baseline configuration ($\zeta = 0.26$). However, the design is stable in both cases.

Finally, the responses of the blade are compared. The plots of the variation of the tip deflection are shown in Fig. 7. It is observed that both designs result in an appreciable change in the steady lag and torsion response. For the flap response, the single-objective and multiobjective results are almost same but show an appreciable change from the baseline. The lag deflection increases for the single-objective case and further increases for the multiobjective case. The torsion response in the multiobjective case is reduced due to high torsion stiffness.

The results in this paper show that metamodels based on orthogonal arrays and second-order response surfaces can be used for obtaining improved designs for rotorcraft optimization problems. However, they do not guarantee a mathematical minima. To get further improvements in the objective function, the points obtained by the OA-based optimization can be used as a starting point for a gradient-based design.

Conclusions

In this paper, the use of response surfaces in building metamodels for rotor design optimization is studied. The objective is to reduce vibratory hub loads and blade root dynamic stresses using blade stiffness design variables. An aeroelastic analysis based on finite elements in space and time and using unsteady aerodynamics and free wake inflow modeling is used. Numerical results are obtained for a soft-inplane, four-bladed hingeless rotor. The following conclusions are drawn from this study:

1) A systematic study of factorial (2^k and 3^k), face-centered CCD, gradient-enhanced CCD, and orthogonal array–based experimental designs is conducted using linear, quadratic, and cubic response surfaces. The different metamodels are compared statistically and through the final optimization results obtained by using them for a vibration reduction problem with three design variables. It is found that the face-centered CCD and orthogonal arrays using quadratic polynomial approximations result in a fairly accurate model compared to other designs, which used more points and/or cubic polynomial approximations.

2) The use of a sequence of second-order polynomial response surfaces with face-centered CCD and orthogonal array–based experimental design yielded similar results in terms of vibration reduction of about 6 and 20% with three and six design variables, respectively. However, the number of analysis code runs needed is appreciably smaller for the orthogonal array design for both three- and six-design-variable cases compared to face-centered CCD.

3) The orthogonal array technique is also used for a multiobjective optimization problem with three objective functions comprising vibratory hub loads, 1/rev blade root loads, and 2/rev blade root loads, which are the principal cause of dynamic stresses. Numerical results obtained using the min–max method and sequential response surfaces show a reduction in the vibratory hub loads of about 16% and in the 1/rev and 2/rev blade root loads of about 18 and 31%, respectively.

4) For the six-variable design, the single-objective (vibratory hub loads) optimization results in a final design that is softer in flap, lag, and torsion compared to the baseline blade and the multiobjective optimization results in a final design that is stiffer in torsion and softer in flap and lag compared to the baseline blade. There is an appreciable change in the lag and torsion response in both cases. However, the least damped regressive lag mode is only marginally affected and the final designs remain aeromechanically stable.

5) Though the results are obtained at an advance ratio of $\mu = 0.3$, a reduction in vibratory hub loads and dynamic stress objective function is also observed at other advance ratios.

It can thus be concluded the the response surface approximation can be used to build accurate approximations to the analysis code using orthogonal array techniques for the design of a low-vibration rotor.

References

[1]Friedmann, P. P., and Hodges, D. H., "Rotary Wing Aeroelasticity—A Historical Perspective," *Journal of Aircraft*, Vol. 40, No. 6, 2003, pp. 1019–1046.

[2]Gandhi, F., and Sekula, M. K., "Helicopter Vibration Reduction Using Fixed-System Auxiliary Moments," *AIAA Journal*, Vol. 42, No. 3, 2004, pp. 501–512.

[3]Riechert, G., "Helicopter Vibration Control—A Survey," *Vertica*, Vol. 5, No. 1, 1981, pp. 1–20.

[4]Loewy, R. G., "Helicopter Vibrations: A Technological Perspective," *Journal of the American Helicopter Society*, Vol. 29, Oct. 1984, pp. 4–30.

[5]Friedmann, P. P., and Millott, T. A., "Vibration Reduction in Rotorcraft Using Active Control, A comparison of Various Approaches," *Journal of Guidance, Control, and Dynamics*, Vol. 18, No. 4, 1995, pp. 664–673.

[6]Chopra, I., "Review of State of Art of Smart Structures and Integrated Systems," *AIAA Journal*, Vol. 40, No. 11, 2002, pp. 2145–2187.

[7]Walsh, J. L., Bingham, G. J., and Riley, M. F., "Optimization Methods Applied to Aerodynamic Design of Helicopter Rotor Blades," *Journal of the American Helicopter Society*, Vol. 32, No. 4, 1987, pp. 928–936.

[8]Friedmann, P. P., and Shanthakumaran, P., "Optimum Design for Rotor Blades for Vibration Reduction in Forward Fight," *Journal of the American Helicopter Society*, Vol. 29, No. 4, 1984, pp. 70–80.

[9]Lim, J. W., and Chopra, I., "Aeroelastic Optimization of a Helicopter Rotor Using Efficient Sensitivity Analysis," *AIAA Journal*, Vol. 28, No. 1, 1991, pp. 29–37.

[10]Ganguli, R., and Chopra, I., "Aeroelastic Optimization of a Helicopter Rotor with Composite Coupling," *Journal of Aircraft*, Vol. 32, No. 6, 1995, pp. 1326–1334.

[11]Venkatesan, C., Friedmann, P. P., and Yuan, K. A., "A New Sensitivity Analysis for Structural Optimization of Composite Rotor Blades," *Mathematical and Computer Modeling*, Vol. 19, No. 3–4, 1994, pp. 1–25.

[12]Sahasrabudhe, V., and Celi, R., "Treatment of Moderate Amplitude Constraints for Handling Qualities Design Optimization," *Journal of Aircraft*, Vol. 34, No. 6, 1997, pp. 730–739.

[13]Fusato, D., and Celi, R., "Design Sensitivity Analysis for Helicopter Fight Dynamic and Aeromechanic Stability," *Journal of Guidance, Control, and Dynamics*, Vol. 26, No. 6, 2003, pp. 918–927.

[14]Shih, I. C., Spence, A. M., and Celi, R., "Semianalytical Sensitivity of Floquet Characteristic Exponents with Application to Rotary-Wing Aeroelasticity," *Journal of Aircraft*, Vol. 33, No. 2, 1996, pp. 322–330.

[15]Chattopadhyay, A., and McCarthy, T. R., "A Multidisciplinary Optimization Approach for Vibration Reduction in Helicopter Rotor Blade Design," *Computer and Mathematics with Applications*, Vol. 25, No. 2, 1993, pp. 59–72.

[16]Kim, J. E., and Sarigul-Klijn, N., "Elastic-Dynamic Rotor Blade Design with Multiobjective Optimization," *AIAA Journal*, Vol. 39, No. 9, 2001, pp. 1652–1661.

[17]Soykasap, O., and Hodges, D. H., "Performance Enhancement of a Composite Tilt-Rotor Using Aeroelastic Tailoring," *Journal of Aircraft*, Vol. 37, No. 5, 2000, pp. 850–858.

[18]Yuan, K. A., and Friedmann, P. P., "Structural Optimization for Vibratory Loads Reduction of Composite Helicopter Rotor Blades with Advanced Geometry Tips," *Journal of the American Helicopter Society*, Vol. 43, No. 3, 1998, pp. 246–256.

[19]Ganguli, R., and Chopra, I., "Aeroelastic Optimization of an Advanced Geometry Rotor," *Journal of the American Helicopter Society*, Vol. 41, No. 1, 1996, pp. 18–28.

[20]Hathaway, E., and Gandhi, F., "Concurrently Optimized Aeroelastic Couplings and Rotor Stiffness for Alleviation of Helicopter Aeromechanical Instability," *Journal of Aircraft*, Vol. 38, No. 1, 2001, pp. 69–80.

[21]Heverly, D. E., Wang, K. W., and Smith, E. C., "An Optimal Actuator Placemnet Methodology for Active Control of Helicopter Airframe Vibrations," *Journal of the American Helicopter Society*, Vol. 46, No. 4, 2001, pp. 251–261.

[22]Zhang, J., Smith, E. C., and Wang, K. W., "Active Passive Hybrid Optimization of Rotor Blades with Trailing Edge Flaps," *Journal of the American Helicopter Society*, Vol. 49, No. 1, 2004, pp. 44–54.

[23]Lee, J., and Hajela, P., "Parallel Genetic Algorithm Implementation in Multidisciplinary Rotor Blade Design," *Journal of Aircraft*, Vol. 33 No. 5, 1996, pp. 962–969.

[24]Crossley, W. A., and Laananen, D. H., "The Genetic Algorithm as an Automated Methodology for Helicopter Conceptual Design," *Journal of Engineering Design*, Vol. 33, No. 6, 1997, pp. 1062–1070.

[25]Ganguli, R., "Survey of Recent Developments in Rotorcraft Design Optimization," *Journal of Aircraft*, Vol. 41, No. 3, 2004, pp. 493–510.

[26]Celi, R., and Friedmann, P. P., "Structural Optimization with Aeroelastic Constraints of Rotor Blades with Straight and Swept Tips," *AIAA Journal*, Vol. 28, No, 3, 1990, pp. 928–936.

[27]Ganguli, R., "Optimum Design of a Helicopter Rotor for Low Vibration Using Aeroelastic Analysis and Response Surface Methods," *Journal of Sound and Vibration*, Vol. 258, No. 2, 2002, pp. 327–344.

[28]Murugan, S. M., and Ganguli, R., "Aeroelastic Stability Enhancement and Vibration Suppression in a Composite Helicopter Rotor," *Journal of Aircraft*, Vol. 42, No. 4, 2005, pp. 1013–1024.

[29]Simpson, T. W., Peplinski, J., Koch, P. N., and Allen, J., "Metamodels for Computer-Based Engineering Design: Survey and Recommendations," *Engineering with Computers*, Vol. 17, No. 2, 2001, pp. 129–152.

[30]Roux, W. J., Stander, N., and Haftka, R. T., "Response Surface Approximations for Structural Optimization," *International Journal of Numerical Methods in Engineering*, Vol. 42, 1998, pp. 517–534.

[31]Venter, G., and Haftka, R. T., "Construction of Response Surface Approximations for Design Optimization," *AIAA Journal*, Vol. 36, No. 12, 1998, pp. 2242–2249.

[32]Chung, H., and Alonso, J. J., "Using Gradients to Construct Response Surface Models for High-Dimensional Design Optimization Problems," AIAA Paper 2001-0922, Jan. 2001.

[33]Romero, V. J., Swiler, L. P., and Giunta, A. A., "Construction of Response Surfaces Based on Progressive Lattice-Sampling Experimental Designs with Application to Uncertainty Propagation," *Structural Safety*, Vol. 26, No. 3, 2004, pp. 201–219.

[34]Unal, R., Braun, R. D., Moore, A. A., and Lepsch, R. A., "Response Surface Model Building Using Orthogonal Arrays for Computer Experiments," *19th Annual International Conference of the International Society of Parametric Analysis*, New Orleans, LA, 1997, pp. 469–481.

[35]Khoei, A. R., Masters, I., and Gethin, D. T., "Design Optimization of Aluminum Recycling Processes Using Taguchi Technique," *Journal of Materials Processing Technology*, Vol. 127, No. 1, 2002, pp. 96–106.

[36]Lee, K.-H., Yi, J.-W., Park, J.-S., and Park, G.-J., "An Optimization Algorithm Using Orthogonal Arrays in Discrete Design Space for Structures," *Finite Elements in Analysis and Design*, Vol. 40, No. 1, 2003, pp. 121–135.

[37]Sacks, J., Welch, W. J., Toby, J. M., and Wynn, H. P., "Design and Analysis of Computer Experiments," *Statistical Science*, Vol. 4, No. 4, 1989, pp. 409–435.

[38]Montgomery, D. C., *Design and Analysis of Experiments*, Wiley, New York, 1997.

[39]Ross, P. J., *Taguchi Techniques for Quality Engineering*, McGraw–Hill, New York, 1995.

[40]Myers, R. H., and Montgomery, D. C., *Response Surface Methodology—Process and Product Optimization Using Designed Experiments*, Wiley, New York, 1995.

[41]Chopra, I., and Bir, G., "University of Maryland Advanced Rotor Code: umarc," *Proceedings of the AHS Aeromechanics Specialists Conference*, American Helicopter Society, Alexandria, VA, 1994, pp. PS.5-1–PS.5-31.

[42]Belegundu, A. D., and Chandrapatla, T. R., *Optimization Concepts and Applications in Engineering*, Pearson Education, Singapore, 2003.

C. Pierre
Associate Editor